

## Strong Dynamical Heterogeneity and Universal Scaling in Driven Granular Fluids

Karina E. Avila,<sup>1,2,\*</sup> Horacio E. Castillo,<sup>1</sup> Andrea Fiege,<sup>3</sup> Katharina Vollmayr-Lee,<sup>4</sup> and Annette Zippelius<sup>3,2</sup>

<sup>1</sup>*Department of Physics and Astronomy and Nanoscale and Quantum Phenomena Institute, Ohio University, Athens, Ohio 45701, USA*

<sup>2</sup>*Max-Planck-Institut für Dynamik und Selbstorganisation, Am Fassberg 17, D-37077 Göttingen, Germany*

<sup>3</sup>*Institut für Theoretische Physik, Georg-August-Universität Göttingen, Friedrich-Hund-Platz 1, D-37077 Göttingen, Germany*

<sup>4</sup>*Department of Physics and Astronomy, Bucknell University, Lewisburg, Pennsylvania 17837, USA*

(Received 18 December 2013; published 10 July 2014)

Large-scale simulations of two-dimensional bidisperse granular fluids allow us to determine spatial correlations of slow particles via the four-point structure factor  $S_4(q, t)$ . Both cases, elastic ( $\epsilon = 1$ ) and inelastic ( $\epsilon < 1$ ) collisions, are studied. As the fluid approaches structural arrest, i.e., for packing fractions in the range  $0.6 \leq \phi \leq 0.805$ , scaling is shown to hold:  $S_4(q, t)/\chi_4(t) = s(q\xi(t))$ . Both the dynamic susceptibility  $\chi_4(\tau_\alpha)$  and the dynamic correlation length  $\xi(\tau_\alpha)$  evaluated at the  $\alpha$  relaxation time  $\tau_\alpha$  can be fitted to a power law divergence at a critical packing fraction. The measured  $\xi(\tau_\alpha)$  widely exceeds the largest one previously observed for three-dimensional (3d) hard sphere fluids. The number of particles in a slow cluster and the correlation length are related by a robust power law,  $\chi_4(\tau_\alpha) \approx \xi^{d-p}(\tau_\alpha)$ , with an exponent  $d - p \approx 1.6$ . This scaling is remarkably independent of  $\epsilon$ , even though the strength of the dynamical heterogeneity at constant volume fraction depends strongly on  $\epsilon$ .

DOI: 10.1103/PhysRevLett.113.025701

PACS numbers: 64.70.Q-, 61.20.Lc, 61.43.Fs

Viscous liquids, colloidal suspensions, and granular fluids are all capable of undergoing dynamical arrest, either by reducing the temperature in the case of viscous liquids or by increasing the density in the cases of colloidal suspensions and of granular systems [1–4]. As the dynamical arrest is approached, not only does the dynamics become dramatically slower, but it becomes increasingly heterogeneous [4–21]. One of the most common ways to characterize the heterogeneity in the dynamics is to probe its fluctuations [4]. Since probing the dynamics requires observing the system at two times, probing the spatial fluctuations in the dynamics naturally leads to defining quantities that correlate the changes in the state of the system between two times, at two spatial points, i.e., four-point functions. Those quantities include the dynamic susceptibility  $\chi_4(t)$ , which gives a spatially integrated measurement of the total fluctuations, and the four-point structure factor  $S_4(q, t)$ , which is the Fourier transform of the spatial correlation function describing the local fluctuations in the dynamics [4,12,15]. From the small wave vector behavior of  $S_4(q, t)$ , a correlation length  $\xi(t)$  can be extracted, and it has been found in simulations of viscous liquids and dense colloidal suspensions that this correlation length grows as dynamical arrest is approached [4,12,15,16]. For granular matter, on the other hand, the jamming transition has been analyzed extensively, but studies on dynamic heterogeneity are few. Two experimental groups have investigated driven  $2d$  granular beds in the context of dynamic heterogeneity. These studies are restricted to small systems of order a few thousand particles [13,14,17–21].  $\chi_4(t)$  has been measured, but spatial correlations have not been investigated systematically due to

small system size. Instead, compact regions of correlated particles are usually assumed,  $\chi_4(t) \sim \xi^d(t)$ , thereby determining a correlation length  $\xi(t)$ .

Here we determine  $\xi$  and  $\chi_4$  independently from  $S_4(q, t)$ —without further assumption. We show that there is indeed a cooperative length scale that grows dramatically as structural arrest is approached: Varying the density by 10% results in an increase in  $\xi$  by a factor  $\sim 20$ . The number of correlated particles is given by  $\chi_4(t)$ , which increases by a factor  $> 10^2$  in the same range of densities. Both  $\xi(t)$  and  $\chi_4(t)$  are well fitted by power law divergencies. Remarkably, size and length scale are related by a robust power law,  $\chi_4(\tau_\alpha) \approx \xi^{d-p}(\tau_\alpha)$  with an exponent  $d - p \approx 1.6$ , implying that the clusters of slow particles are neither compact nor stringlike. For fixed packing fraction the strength of the dynamical heterogeneity changes dramatically with the degree of inelasticity; however, the scaling  $\chi_4(\tau_\alpha) \approx \xi^{d-p}(\tau_\alpha)$  and the exponent  $d - p$  are universal. To obtain these results, and in particular a correlation length as large as 72 particle radii, we rely on large-scale simulations with typically  $4 \times (10^5 - 10^6)$  particles. We find that in  $2d$  the spatial fluctuations are much stronger but the relaxation time grows much more slowly with length scale than in  $3d$ .

We consider a bidisperse system of hard disks in  $2d$ , with radii  $r_2$  and  $r_1$  such that  $r_2 \approx 1.43r_1$ . The hard disks interact via two-body inelastic collisions: The normal component of the relative velocity of two colliding particles is multiplied by a factor  $\epsilon \leq 1$ , the coefficient of restitution. In the inelastic case  $\epsilon < 1$ , energy  $\propto (1 - \epsilon^2)$  is dissipated in each collision, and has to be supplied in order to reach a steady state. Here, we kick the particles randomly, comparably to

the bulk driving in the experiments presented in Refs. [13,14]. The total injected power is chosen  $\propto (1 - \varepsilon^2)$ , in order to achieve approximately the same granular temperature  $T_G$  (a measure of the rms velocity fluctuations), for all  $\varepsilon$ . The system presented here is the same as the one in Ref. [22], where additional simulation details can be found.

In this work, we analyze simulations for  $\varepsilon = 0.90$  with packing fractions  $0.6 \leq \phi \leq 0.805$ , and for  $\varepsilon = 0.70, 0.80, 1.00$  with packing fractions  $0.72 \leq \phi \leq 0.79$ . The system contains  $N_{\text{tot}} = 4\,000\,000$  particles for  $0.60 \leq \phi \leq 0.78$  and  $N_{\text{tot}} = 360\,000$  particles for  $0.79 \leq \phi \leq 0.805$ . We measure lengths in units of the radius  $r_1$  of the small disks and choose units of time such that  $T_G = 1$ . To analyze the results, we divide the simulation box, which has total area  $L_{\text{tot}}^2$ , into sub-boxes of equal areas  $L^2$ . The number of particles  $N_{\mathbf{r}}$  in each sub-box  $B_{\mathbf{r}}$  (centered at point  $\mathbf{r}$ ) fluctuates over time and between different sub-boxes, but its average  $N = N_{\text{tot}}(L/L_{\text{tot}})^2$  has been kept fixed for each measurement. For all analyses, we select the time window so that the system is in a steady state.

To probe the dynamics, we define the single-particle overlap function  $w_i(t_2, t_1) \equiv \theta(a - |\mathbf{r}_i(t_2) - \mathbf{r}_i(t_1)|)$ , where  $\theta$  is the Heaviside function,  $t_1$  and  $t_2$  are times such that  $t_2 \geq t_1$ ,  $\mathbf{r}_i(t)$  is the position of particle  $i$  at time  $t$ , and  $a$  is the cutoff length. Intuitively, this observable distinguishes between “slow” particles, with  $w_i = 1$ , and “fast” particles, with  $w_i = 0$ . For each sub-box  $B_{\mathbf{r}}$  and for a given time interval between  $t_0$  and  $t_0 + t$  ( $t > 0$ ), we also define the sub-box overlap  $Q_{\mathbf{r}}(t; t_0) = 1/N_{\mathbf{r}} \sum_{i=1}^{N_{\mathbf{r}}} w_i(t_0 + t, t_0)$ , where the sum runs over the particles present in the box  $B_{\mathbf{r}}$  at time  $t_0$ .  $Q_{\mathbf{r}}(t; t_0)$  can be interpreted as the fraction of slow particles in sub-box  $B_{\mathbf{r}}$  in the time interval  $[t_0, t_0 + t]$ .

The average dynamics is characterized by the quantity  $\langle Q_{\mathbf{r}}(t; t_0) \rangle$ , where  $\langle \dots \rangle$  denotes an average over sub-boxes, and  $\overline{\dots}$  denotes an average over initial times  $t_0$  at fixed time difference  $t$ . This quantity exhibits critical slowing down as the packing fraction increases [23]. In particular, the  $\alpha$  relaxation time  $\tau_\alpha$ , defined by  $\langle Q_{\mathbf{r}}(\tau_\alpha; t_0) \rangle = 1/e$ , is a rapidly increasing function of  $\phi$  [23]. Unless otherwise indicated, the results shown below are for  $\varepsilon = 0.9$ ,  $a = 0.6r_1$ , and  $t = \tau_\alpha$ .

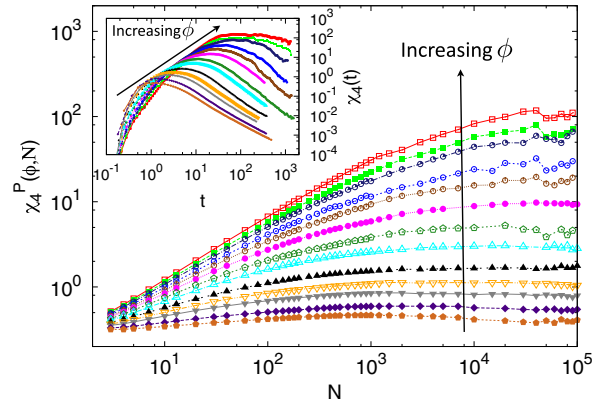


FIG. 1 (color online). Peak value of the dynamic susceptibility  $\chi_4^P$  versus  $N$  for packing fractions  $0.60 \leq \phi \leq 0.805$ . Inset: Dynamic susceptibility  $\chi_4(t)$  for the same packing fractions as in the main panel, for  $N = 10\,000$ .

To quantify the heterogeneity of the dynamics, we use the dynamic susceptibility

$$\chi_4(t) = N[\overline{\langle Q_{\mathbf{r}}^2(t; t_0) \rangle} - \langle Q_{\mathbf{r}}(t; t_0) \rangle^2], \quad (1)$$

which gives a direct measure of the strength of the fluctuations in the overlap. As a function of time,  $\chi_4(t)$  has a maximum  $\chi_4^P$  at time  $\tau^*$ . Both the maximum value  $\chi_4^P$  and its position  $\tau^*$  are increasing functions of the packing fraction  $\phi$  (see Fig. 1, inset). Moreover, as shown in Fig. 1, as a function of  $N$ ,  $\chi_4^P$  initially increases and then reaches a plateau. Both the value of  $N$  at which the plateau starts and the plateau value of  $\chi_4^P$  are increasing functions of the packing fraction  $\phi$ , consistent with the presence of a correlation length  $\xi$  that controls the finite size scaling behavior of  $\chi_4^P$  and that grows with increasing  $\phi$  [24]. To minimize finite size effects, in what follows all results are reported for  $N = 10\,000$  for  $\phi \leq 0.76$  and  $N = 40\,000$  for  $\phi > 0.76$ , which are within the plateau region for all packing fractions considered.

Spatial correlations of the dynamical fluctuations are encoded in the four-point structure factor

$$S_4(q, t)/N = \{[\overline{\langle W_{\mathbf{r}}(\mathbf{q}, t; t_0) W_{\mathbf{r}}(-\mathbf{q}, t; t_0) \rangle} - \langle W_{\mathbf{r}}(\mathbf{q}, t; t_0) \rangle \langle W_{\mathbf{r}}(-\mathbf{q}, t; t_0) \rangle]\}, \quad (2)$$

where  $W_{\mathbf{r}}(\mathbf{q}, t; t_0) = 1/N_{\mathbf{r}} \sum_{i=1}^{N_{\mathbf{r}}} \exp[i\mathbf{q} \cdot \mathbf{r}_i(t_0)] w_i(t_0 + t, t_0)$ , and  $\{\dots\}$  denotes an average over wave vectors  $\mathbf{q}$  of fixed magnitude  $|\mathbf{q}| = q$ . The four-point structure factor and the dynamic susceptibility are related by  $\lim_{q \rightarrow 0} S_4(q, t) = \chi_4(t)$  [25].

As the packing fraction is increased to the point of structural arrest, we expect long-range correlations of the dynamic heterogeneities as well as scaling of  $S_4(q, t)$ .

In Fig. 2 we plot  $S_4(q, \tau_\alpha)/\chi_4(\tau_\alpha)$  as a function of  $q\xi(\tau_\alpha)$ , and find good collapse between data for different  $\phi$ . This shows that all dependence on  $\phi$  can be absorbed into a single length scale, the dynamic correlation length  $\xi(t)$  evaluated at  $\tau_\alpha$ .  $\xi(t)$  can be extracted either by collapsing the data in the scaling plot or by fitting  $S_4(q, t)$  to the Ornstein-Zernicke (OZ) form,  $S_4(q, t) = \chi_4(t)/\{1 + [q\xi(t)]^2\}$ .

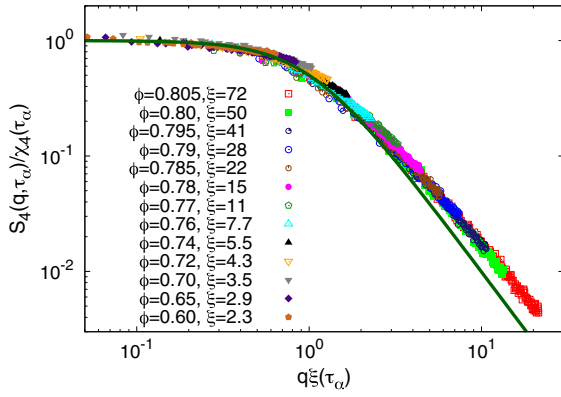


FIG. 2 (color online). Scaling plot of the four-point structure factor  $S_4(q, \tau_\alpha)$  for different packing fractions, with Ornstein-Zernicke fit (solid line). The correlation lengths  $\xi$  are shown in the key.

As can be seen in Fig. 2, the scaling function is close to the OZ form for  $q\xi(\tau_\alpha) \lesssim 1$ , but starts to differ significantly from it for larger values of  $q\xi(\tau_\alpha)$ . The values of  $\xi(\tau_\alpha)$ , reported in Fig. 2, are obtained by fitting  $S_4(q, t)$  to the OZ form in the range  $0 < q < 0.2$ . Changing the fitting range or adding a quartic term to the denominator in the fitting function [16,28] does not significantly alter the results for  $\xi(\tau_\alpha)$  [23].

In Fig. 3, we show that both  $\chi_4(\tau_\alpha)$  and  $\xi(\tau_\alpha)$  grow rapidly with  $\phi$ . In fact, both quantities and also the relaxation time  $\tau_\alpha$  (not shown) are well fitted by divergent power law forms  $\chi_4(\tau_\alpha) \propto (\phi_J - \phi)^{-\gamma_\chi}$ ,  $\xi(\tau_\alpha) \propto (\phi_J - \phi)^{-\gamma_\xi}$ , and  $\tau_\alpha \propto (\phi_J - \phi)^{-\gamma_\tau}$ , with a common location  $\phi_J \approx 0.82$  for all three divergences but different exponents  $\gamma_\chi \approx 2.5$ ,  $\gamma_\xi \approx 1.6$ , and  $\gamma_\tau \approx 2.4$  [23].

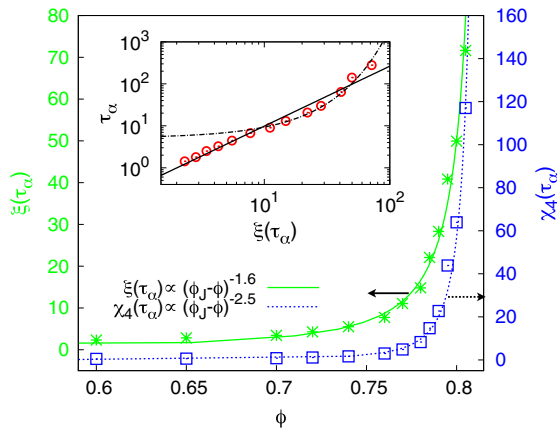


FIG. 3 (color online). The dynamic correlation length  $\xi(\tau_\alpha)$  and the dynamic susceptibility  $\chi_4(\tau_\alpha)$  as functions of the packing fraction  $\phi$ . In each case, a fit to a diverging power law function is shown. Inset: Relaxation time  $\tau_\alpha$  versus dynamic correlation length  $\xi(\tau_\alpha)$ . Two fits to the data are attempted: a power law (solid line) and an exponential (dot-dashed line).

The above results imply a power law relation between time scales and length scales:  $\tau_\alpha \propto [\xi(\tau_\alpha)]^z$ , with a dynamical exponent  $z = \gamma_\tau / \gamma_\xi$ . In the inset of Fig. 3 we show  $\tau_\alpha$  as a function of  $\xi(\tau_\alpha)$ . A power law fit with an exponent  $z = \gamma_\tau / \gamma_\xi \approx 1.5$  is shown (full line), together with an alternative description [16], i.e.,  $\tau_\alpha \propto \exp[k\xi(\tau_\alpha)]$  (dot-dashed line). We do not observe the dramatic slowdown of growth of the correlation volume for very long time scales seen in structural glasses [29,30], although we cannot exclude it happening at length scales that exceed the observed correlation length of 35 particle diameters. This slowdown in glasses is necessary to avoid unphysically large correlation lengths, when extrapolated to experimental time scales, but, in a granular fluid, the time scales are macroscopic and hence time and length scale in the simulation are comparable to experiment.

We now examine how the dynamic susceptibility  $\chi_4(\tau_\alpha)$  and the correlation length  $\xi(\tau_\alpha)$  depend on  $a$ . For  $a$  within the range  $0.2r_1 \leq a \leq 4.0r_1$ , both quantities display the same behavior [31]. They grow monotonically with  $a$ , and three regimes can be identified: extremely fast growth for  $r/a_1 \lesssim 1$ , much slower growth for  $r/a_1 \gtrsim 1$ , and a cross-over in between. Figure 4 shows this for the case of  $\xi(\tau_\alpha)$ . We also find that for fixed  $a$ , the relation between the two quantities is well fitted by a power law,  $\chi_4(\tau_\alpha) \propto \xi^{d-p}(\tau_\alpha)$ , with an exponent  $d-p \approx 1.6$ , which is approximately constant as a function of  $a$ . In the inset of Fig. 4 we show this relation for  $a/r_1 = 0.6, 1.4, 3.0$ , i.e., for one value of  $a$  in each of the regimes described above.

The exponent  $d-p$  gives information about the correlated slow regions. In the most common interpretation,  $d-p$  is the fractal dimension  $d_f$  of those regions. The value  $d_f \approx 1.6$  differs from the expected values for compact domains ( $d_f = 2$ ) and for stringlike domains ( $d_f = 1$ ). It has been suggested that alternatively the correlated regions could be compact, but their sizes could have a wide

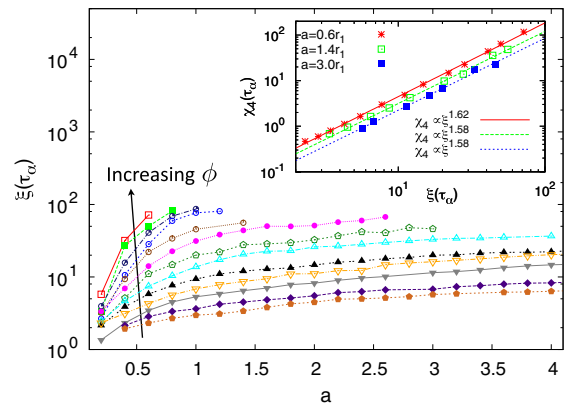


FIG. 4 (color online).  $\xi(\tau_\alpha)$  versus  $a$  for  $0.60 \leq \phi \leq 0.805$  (from bottom to top). Inset:  $\chi_4(\tau_\alpha)$  versus  $\xi(\tau_\alpha)$  for three different choices of the parameter  $a$ . The different lines correspond to the fit  $\chi_4(\tau_\alpha) \propto \xi^{d-p}(\tau_\alpha)$  for each  $a$ .

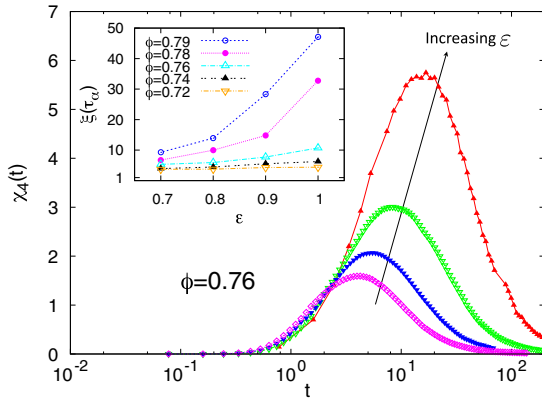


FIG. 5 (color online).  $\chi_4(t)$  for coefficients of restitution  $\varepsilon = 0.70, 0.80, 0.90, 1.00$  ( $\phi = 0.76$  fixed). Inset: Correlation length  $\xi(\tau_\alpha)$  as a function of  $\varepsilon$ , for  $0.72 \leq \phi \leq 0.79$ .

distribution [4,32]. However, this is not compatible with the OZ form of  $S_4(q, t)$ , which implies a fast decay of  $G_4(r, t)$  for large distances  $r$ . We have studied a wide range of values of the cutoff  $a$ , which goes from being barely larger than the typical displacement associated with vibrations of caged particles to being larger than the displacement required to reach the position of second neighbors to the original location of the particle. Therefore, it is remarkable that the exponent  $d - p$  is essentially constant over this whole range of values of  $a$ .

We now turn to the analysis of the effects of dissipation by comparing results for different values of the coefficient of restitution  $\varepsilon$ . In Fig. 5 we show the dynamic susceptibility  $\chi_4(t)$  for  $\phi = 0.76$  and  $\varepsilon = 0.70, 0.80, 0.90$ , and  $1.00$  (elastic). As  $\varepsilon$  grows, the height of the peak of  $\chi_4(t)$  increases and the peak shifts to longer times. In the inset we show that  $\xi(\tau_\alpha)$  also grows as a function of  $\varepsilon$  and that this growth is stronger for higher packing fractions. Both results are compatible with an  $\varepsilon$ -dependent critical density  $\phi_J(\varepsilon)$  as predicted in Ref. [33]. Such a shift in the critical density

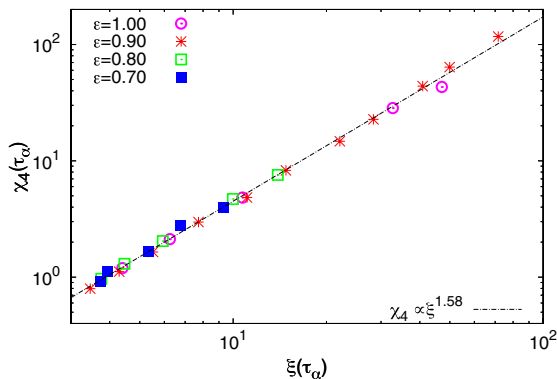


FIG. 6 (color online).  $\chi_4(\tau_\alpha)$  against  $\xi(\tau_\alpha)$  for  $0.70 \leq \varepsilon \leq 1.00$  and  $0.72 \leq \phi \leq 0.79$ . All data are fitted to  $\chi_4(\tau_\alpha) \propto \xi^{d-p}(\tau_\alpha)$ , with  $d - p \approx 1.59$  (dot-dashed line).

drops out if we plot the relation between  $\chi_4(\tau_\alpha)$  and  $\xi(\tau_\alpha)$ , as is done in Fig. 6 for  $\varepsilon = 0.70, 0.80, 0.90$ , and  $1.00$ . We find that a single power law  $\chi_4(\tau_\alpha) \propto \xi^{d-p}(\tau_\alpha)$ , with  $d - p \approx 1.6$ , provides a good fit for the data corresponding to all values of  $\varepsilon$ . In fact, attempting separate fits for each  $\varepsilon$  leads to obtaining exponents that are equal to each other within error bars.

In summary, we studied dynamical heterogeneity in a 2d driven granular fluid in the range of packing fractions  $0.6 \leq \phi \leq 0.805$ . The four-point dynamic structure factor was shown to obey scaling,  $S_4(q, \tau_\alpha)/\chi_4(\tau_\alpha) = s(q\xi(\tau_\alpha))$ , where the scaling function is well fitted by the Ornstein-Zernicke form for small argument. This allowed us to determine the dynamic susceptibility  $\chi_4(\tau_\alpha)$  and the correlation length  $\xi(\tau_\alpha)$  independently. Both were shown to grow dramatically with the packing fraction  $\phi$  and can be well fitted by divergent power laws within the range of packing fractions accessible to our simulations. For restitution coefficients  $0.7 \leq \varepsilon \leq 1.0$ , and a wide range of cutoffs  $0.6 \leq a/r_1 \leq 3.0$ , we found a robust scaling  $\chi_4(\tau_\alpha) \propto \xi^{d-p}(\tau_\alpha)$ , with  $d - p \approx 1.6$ , implying that the correlated regions are neither stringlike nor compact. We conclude that the observed scaling of dynamical heterogeneities is remarkably universal with respect to dissipation and much stronger in 2d than in 3d.

H. E. C. thanks E. Flenner and G. Szamel for discussions. This work was supported in part by DFG under Grants No. SFB 602 and No. FOR 1394, by DOE under Grant No. DE-FG02-06ER46300, by NSF under Grants No. PHY99-07949 and No. PHY05-51164, and by Ohio University. K. E. A. acknowledges the CMSS program at Ohio University for partial support. We thank I. Gholami and T. Kranz for help with the numerical simulations.

\*karina.avila@theorie.physik.uni-goettingen.de

- [1] P. G. Debenedetti and F. H. Stillinger, *Nature (London)* **410**, 259 (2001).
- [2] P. N. Pusey and W. van Meegen, *Nature (London)* **320**, 340 (1986).
- [3] C. S. O'Hern, L. E. Silbert, A. J. Liu, and S. R. Nagel, *Phys. Rev. E* **68**, 011306 (2003).
- [4] *Dynamical Heterogeneities in Glasses, Colloids and Granular Materials*, edited by L. Berthier, G. Biroli, J.-P. Bouchaud, L. Cipelletti, and W. van Saarloos (Oxford University Press, Oxford, England, 2011).
- [5] M. D. Ediger, *Annu. Rev. Phys. Chem.* **51** 99 (2000).
- [6] H. Sillescu, *J. Non-Cryst. Solids* **243**, 81 (1999).
- [7] E. Vidal Russell and N. E. Israeloff, *Nature (London)* **408**, 695 (2000).
- [8] W. K. Kegel and A. van Blaaderen, *Science* **287**, 290 (2000).
- [9] E. R. Weeks, J. C. Crocker, A. C. Levitt, A. B. Schofield, and D. A. Weitz, *Science* **287**, 627 (2000).
- [10] L. Cipelletti, H. Bissig, V. Trappe, P. Ballesta, and S. Mazoyer, *J. Phys. Condens. Matter* **15**, S257 (2003).

- [11] B. Doliwa and A. Heuer, *Phys. Rev. E* **61**, 6898 (2000).
- [12] N. Lačević, F. W. Starr, T. B. Schröder, and S. C. Glotzer, *J. Chem. Phys.* **119**, 7372 (2003).
- [13] A. R. Abate and D. J. Durian, *Phys. Rev. E* **76**, 021306 (2007).
- [14] A. S. Keys, A. R. Abate, S. C. Glotzer, and D. J. Durian, *Nat. Phys.* **3**, 260 (2007).
- [15] C. Toninelli, M. Wyart, L. Berthier, G. Biroli, and J.-P. Bouchaud, *Phys. Rev. E* **71**, 041505 (2005).
- [16] E. Flenner, M. Zhang, and G. Szamel, *Phys. Rev. E* **83**, 051501 (2011).
- [17] O. Dauchot, G. Marty, and G. Biroli, *Phys. Rev. Lett.* **95**, 265701 (2005).
- [18] G. Marty and O. Dauchot, *Phys. Rev. Lett.*, **94**, 015701 (2005).
- [19] R. Candelier, O. Dauchot, and G. Biroli, *Phys. Rev. Lett.* **102**, 088001 (2009).
- [20] F. Lechenault, O. Dauchot, G. Biroli, and J. P. Bouchaud, *Europhys. Lett.* **83**, 46003 (2008).
- [21] F. Lechenault, O. Dauchot, G. Biroli, and J. P. Bouchaud, *Europhys. Lett.* **83**, 46002 (2008).
- [22] I. Gholami, A. Fiege, and A. Zippelius, *Phys. Rev. E* **84**, 031305 (2011).
- [23] K. E. Avila, H. E. Castillo, A. Fiege, K. Vollmayr-Lee, and A. Zippelius (to be published).
- [24] S. Karmakar, C. Dasgupta, and S. Sastry, *Proc. Natl. Acad. Sci. U.S.A.* **106** 3675 (2009).
- [25] In most numerical simulations, in which the particle density and the relative concentrations of each particle type are held fixed, a correction term is needed in  $\lim_{q \rightarrow 0} S_4(q, t) = \chi_4(t)$  [16,26,27]. In the present work, however, as particles are exchanged between sub-boxes, the particle density and the relative concentrations in each sub-box do fluctuate, and for each sub-box the rest of the system can be thought of as a particle reservoir. Therefore, no correction term is needed. We have tested this statement with our data and found that it holds within statistical error.
- [26] J. L. Lebowitz, J. K. Percus, and L. Verlet, *Phys. Rev.* **153**, 250 (1967).
- [27] L. Berthier, G. Biroli, J.-P. Bouchaud, L. Cipelletti, D. Masri, D. L'Hôte, F. Ladieu, and M. Pierno, *Science* **310**, 1797 (2005).
- [28] S. Karmakar, C. Dasgupta, and S. Sastry, *Phys. Rev. Lett.* **105**, 015701 (2010).
- [29] C. Dalle-Ferrier, C. Thibierge, C. Alba-Simionesco, L. Berthier, G. Biroli, J.-P. Bouchaud, F. Ladieu, D. L'Hôte, and G. Tarjus, *Phys. Rev. E* **76**, 041510 (2007).
- [30] P. Harrowell, in *Dynamical Heterogeneities in Glasses, Colloids and Granular Materials (Ref. 4)* (Oxford University Press, Oxford, England, 2011).
- [31] In a comparable experiment, Abate and Durian [13] find that the maximum dynamic susceptibility  $\chi_4^p$  at fixed  $\phi$  first increases with increasing  $a$ , then reaches a maximum for  $a = a_{\max} \approx 2.2r_1$ , and then decreases for larger  $a$ . It is possible that a similar maximum could appear in our simulations for a value of  $a_{\max}$  larger than  $4.0r_1$ , but we cannot address that question with the data available.
- [32] One way in which  $d - p < 2$  could be obtained, even if the cluster fractal dimension  $d_f$  is very close to 2, is if the distribution of cluster linear sizes  $\hat{\xi}$  has a power law tail with a cutoff  $\rho(\hat{\xi}) \propto \theta(\hat{\xi}_{\max} - \hat{\xi})\hat{\xi}^{-\alpha}$ , with  $\alpha = 3 - (2/p)(2 - d_f)$  [23]. In particular,  $d - p = 1.6$  would correspond to  $\alpha = 3 - 5(2 - d_f)$ . This is based on the assumption that the correlation length  $\xi$  that is extracted from the small  $q$  limit of  $S_4(q, t)$  is an estimate of the rms value  $\xi = \langle \hat{\xi}^2 \rangle^{1/2}$ .
- [33] W. T. Kranz, M. Sperl, and A. Zippelius, *Phys. Rev. Lett.* **104**, 225701 (2010); *Phys. Rev. E* **87**, 022207 (2013).